ON-WAFER NOISE FIGURE CHARACTERIZATION FOR RADIO FREQUENCY INTEGRATED CIRCUITS

SHUKRI KORAKKOTTIL KUNHI MOHD

UNIVERSITI SAINS MALAYSIA
2011

ON-WAFER NOISE FIGURE CHARACTERIZATION FOR RADIO FREQUENCY INTEGRATED CIRCUITS

by

SHUKRI KORAKKOTTIL KUNHI MOHD

Thesis submitted in fulfilment of the requirements
for the degree of
Master of Science

MARCH 2011

DECLARATION

I hereby declare that the work in this thesis is my own except for quotations and summaries which have been duly acknowledged.

7^{th} March 2011 Shukri Korakkottil Kunhi Mohd

P-LM0317

ACKNOWLEDGMENTS

In the name of Allah, the most gracious and the most merciful. First and foremost I offer my sincerest gratitude to my supervisor, Associate Professor Dr Tun Zainal Azni Zulkifli, who has supported me with his patience and knowledge throughout my thesis. I attribute my accomplishment to his encouragement and effort and without him this thesis would not have been completed. One simply could not wish for a better and friendlier supervisor as he is. His many suggestions and advices had triggered ideas that had helped me in many times of despair when my research were facing some problems.

I also owe my sincerest gratitude to Associate Professor Dr Othman Sidek as my co-supervisor who offers me the opportunity to work at the Collaborative Microelectronic Design Excellence Center (CEDEC), where I've also been given the privilege to use the test and measurement facilities. My gratitude also goes to other members of CEDEC who were involved directly or indirectly in this research work.

My appreciation also goes to the School of Electrical and Electronic Engineering (SEEE), USM for giving me the opportunity to further my studies at the masters' level, as well as to all in SEEE who were involved in this work. Many thanks to members of Radio Frequency and Mixed Signal Integrated Circuit (RMIC) group for their support and also for very helpful discussions.

Finally, my gratitude to the person who matters to me most, my wife, Mrs. Noraini Dollah. Being with her serves as a motivation towards the completion of my studies. This project was partially supported by MOSTI grant no. 03-01-05-SF0302, MOHE grant no. 6071146 and Short Term grant no. 6039029.

TABLE OF CONTENTS

Index 89

LIST OF TABLES

LIST OF FIGURES

LIST OF ABBREVIATIONS

ACP Air Coplanar Probes

AH Angka Hingar

DC Direct Current

DUT Device Under Test

dB Decibel

ENR Excess Noise Ratio

F Noise Factor

FR Frekuensi Radio

GPIB General Purpose Input/Output

GPS Global Positioning System

IC Integrated Circuits

IP Intellectual Property

ISS Impedance Standard Substrate

LBFR Litar Bersepadu Frekuensi Radio

LNA Low-Noise Amplifier

MOS Metal Oxide Semiconductor

NF Noise Figure

NFA Noise Figure Analyzer

SPA Semiconductor Parameter Analyzer

PCB Printed Circuit Board

PDU Peranti Dibawah Ujian

PHR Penguat Hingar Rendah

RF Radio Frequency

RFIC Radio Frequency Integrated Circuit

RFID Radio Frequency Identification

RMIC Radio Frequency and Mixed-Signal Integrated Circuit

RMS Root Mean Square

SKG Sistem Kedudukan Global

SMA SubMiniature version A

SNR Signal-to-Noise Ratio

SOLT Short-Open-Load-Thru

USB Universal Seral Bus

USM Universiti Sains Malaysia

VNA Vector Network Analyzer

LIST OF SYMBOLS

a constant (in MOSFET devices, ‘a’ refers to g_m)

c intercept points at y-axis

b constant (in MOSFET devices, ‘b’ refers to ‘W,’ ‘L’ and ‘C_{ox}’)

$c1$ constant in the range 0.5 to 2

Δf bandwidth

Ω Ohm

f frequency (Hz)

F_1 noise factor of the first stage

F_2 noise factor of the second stage

F_{all} noise factor of all the stages

f_c particular frequency for a given noise process

F_{DUT} noise factor of the device under test

F_{IN} noise factor of the input stage

F_{NFA} noise factor of the noise figure analyzer

F_{OUT} noise factor of the output stage

G gain

G_1 gain of the first stage

G_2 gain of the second stage

G_a available gain

Γ_{OUT} reflection coefficient of the output stage

Γ_S reflection coefficient of the noise source

G_{DUT} gain of the device under test

G_i insertion gain

G_{IN} gain of the input stage

G_{OUT} gain of the output stage

I Current (A)

I_{DC} current flow through a device

k boltzmann's constant, which is equal to $(1.38 \times 10^{-23})(J/K)$

K_1 constant for particular device

K_2 constant for particular device

m slope of the graph

N_1 noise output power during the 'COLD' state

N_2 noise output power during the 'HOT' state

N_1^0 noise output power during the 'COLD' state without device under test

N_2^0 noise output power during the 'HOT' state without device under test

N_i available noise power at the input of a device

N_{i1} small amount of thermal noise during the ‘COLD’ state

N_{i2} large amount of thermal noise during the ‘HOT’ state

N_o available noise power at the output of a device

N_a noise power added by a device

N_{a1} noise power added by a device in the first stage

N_{a2} noise power added by a device in the second stage

N_{o1} available noise power at the output for the first stage

N_{o2} available noise power at the output for the second stage

P Power

q quantum

R resistor

S_{11} input reflection coefficient

S_{21} forward transmission coefficient

S_{12} reverse transmission coefficient

S_{22} output reflection coefficient

S_{11}^{OPEN} input reflection coefficient, which measured when the input stage is connected to the‘OPEN’ standard

S_{11}^{SHORT} input reflection coefficient, which measured when the input stage is connected to the ‘SHORT’ standard

S_{11}^{LOAD} input reflection coefficient, which measured when the input stage is connected to the 'LOAD' standard

S_{22}^{OPEN} output reflection coefficient, which measured when the output stage is connected to the 'OPEN' standard

S_{22}^{SHORT} output reflection coefficient, which measured when the output stage is connected to the 'SHORT' standard

S_{22}^{LOAD} output reflection coefficient, which measured when the output stage is connected to the 'LOAD' standard

S_{11}^{IN} input reflection coefficient of the input stage

S_{21}^{IN} forward transmission coefficient of the input stage

S_{12}^{IN} reverse transmission coefficient of the input stage

S_{22}^{IN} output reflection coefficient of the input stage

S_{11}^{OUT} input reflection coefficient of the output stage

S_{21}^{OUT} forward transmission coefficient of the output stage

S_{12}^{OUT} reverse transmission coefficient of the output stage

S_{22}^{OUT} output reflection coefficient of the output stage

S_{11}^{DUT} input reflection coefficient of the device under test

S_{21}^{DUT} forward transmission coefficient of the device under test

S_{12}^{DUT} reverse transmission coefficient of the device under test

S_{22}^{DUT} output reflection coefficient of the device under test

S_i available signal power at the input

S_o available signal power at the output

T temperature (K)

T_c temperature of noise source during the ‘COLD’ state (K)

T_h temperature of noise source during the ‘HOT’ state (K)

T_o reference temperature (K)

v_n noise voltage

i_n noise current

x x-axis

y y-axis

PUBLICATION

S. Korakkottil Kunhi Mohd, T. Z. A. Zulkifli and O. Sidek, “A general on-wafer noise figure de-embedding technique with gain uncertainty analysis", *IEICE Electron. Express*, Vol. 7, No. 4, pp. 302-307, (2010).

PENCIRIAN ANGKA HINGAR ATAS-WAFER UNTUK LITAR BERSEPADU FREKUENSI RADIO

ABSTRAK

Kaedah nyah-benaman pengukuran Angka Hingar (AH) atas-wafer untuk Litar Bersepadu Frekuensi Radio (LBFR) dibentangkan dalam tesis ini. Ini diikuti dengan analisa ketakpastian gandaan untuk menyiasat pengaruh pengukuran skalar dan vektor terhadap AH. Dalam tesis ini, semua unsur yang terlibat ditentukan dan dikategorikan sebagai sistem berbilang tahapan. Kabel dan kuar masukan serta kabel dan kuar keluaran masing-masing dikategorikan sebagai tahapan masukan dan keluaran. Kemudian, parameter-S untuk setiap tahapan tersebut diukur dengan menggunakan pendekatan kaedah pengukuran parameter-S satu liang. Seterusnya, persamaan Friis yang terkenal diaplikasi untuk membetulkan sumbangan hingar yang datang dari setiap tahapan tersebut. Dalam erti kata untuk mengesahkan kaedah yang dicadangkan ini, prosedur nyah-benaman tersebut diaplikasikan pada rekabentuk rujukan, dimana Penguat Hingar Rendah (PHR) model MAX2654 dari Maxim Integrated Products digunakan. MAX2654 mempunyai spesifikasi AH sebanyak 1.5 dB pada 1.575 GHz. Pada frekuensi operasi, perbezaan sebanyak 0.17 dB diperoleh dengan membandingkan AH yang tercatat dalam spesifikasi rekabentuk rujukan dengan keputusan pengukuran menggunakan prosedur nyah-benaman. Berlawanan dengan perbezaan sebanyak 1.8 dB diperolehi tanpa prosedur nyah-benaman, proses pengesahan terse-

but telah membuktikan kaedah yang dicadangkan ini boleh menyumbang kepada pengukuran AH atas-wafer yang lebih jitu. Prosedur nyah-benaman tersebut kemudiannya diaplikasikan pada sumber induktif ternyahjana PHR yang direkabentuk untuk aplikasi Sistem Kedudukan Global (SKG) dengan frekuensi operasi pada 1.44 GHz. AH 3.8 dB diperoleh dengan prosedur nyah-benaman, yang mana lebih rendah dari 6.06 dB yang diperoleh tanpa menggunakan prosedur nyah-benaman. Untuk analisis ketakpastian, AH yang diperoleh dengan pengukuran skalar melalui penggunaan gandaan sisipan (G_i) dibandingkan dengan AH yang diperoleh dengan gandaan boleh dapat (G_a) menerusi pengukuran vektor. Berlainan pengukuran skalar, keadaan pemadanan Peranti Dibawah Ujian (PDU) akan dipertimbangkan dengan penggunaan pengukuran vektor. Keputusan pengukuran AH menerusi G_a menunjukkan pembaikan sebanyak 0.18 dB jika dibandingkan dengan pengukuran AH menggunakan G_i, yang mana menunjukkan pemadanan mempunyai pengaruh besar pada pengukuran AH. Akhir sekali, kesan pemadanan terhadap AH dianalisa. Analisa ini dibuat dengan memperkenalkan tiga galangan piawai keatas PDU untuk memberikan keadaan pemadanan yang berbeza. Untuk situasi tersebut, AH diukur pada 5.63 dB, 5.76 dB, dan 4.75 dB yang mana masing-masing adalah untuk galangan ‘PINTAS’, ‘BUKA’, dan ‘BEBAN’.

ON-WAFER NOISE FIGURE CHARACTERIZATION FOR RADIO FREQUENCY INTEGRATED CIRCUITS

ABSTRACT

A de-embedding method of an on-wafer Noise Figure (NF) measurement for Radio Frequency Integrated Circuit (RFIC) is presented in this thesis. This is then followed by gain uncertainty analysis to investigate the influences of scalar and vector measurements on the NF. As implemented in this thesis, all elements involved in the setup were determined and classified as a multi-stage system. Input cable and probe as well as output cable and probe were both grouped into input and output stages, respectively. Then, S-parameter for these input and output stages were measured using one-port S-parameter measurement approach. Next, a well known Friis equation was applied to correct the noise contributions coming from these stages. In order to validate the proposed method, the de-embedding procedure was applied on a reference design, where Low-Noise Amplifier (LNA) modeled MAX2654 from Maxim Integrated Products was used. MAX2654 has the specification of 1.5 dB NF at 1.575 GHz. At the frequency of operation, a difference of 0.17 dB attained by comparing Noise Figure (NF) specification of reference design and the result of measurement that using the de-embedding procedure. As opposed to 1.8 dB difference obtained without the de-embedding method, the validation process has proven that the proposed method contributes to a more accurate on-wafer NF measurement. The de-embedding proce-

dure is then applied on the inductively source degenerated LNA designed for Global Positioning System (GPS) application with the frequency of operation at 1.44 GHz. NF of 3.8 dB achieved using the de-embedding procedure, which is lower than the 6.06 dB without the de-embedding procedure. As for the uncertainty analyses, NF obtained with a scalar measurement through the use of an insertion gain (G_i) was compared to the NF obtained with an available gain (G_a), utilizing a vector measurement. Unlike scalar measurement, matching conditions of the DUT were encountered by utilizing the vector measurement instead. Results for the NF measurement using G_a shows 0.18 dB improvement as compared to the NF measurement using G_i, which shows that matching has great influences on the NF measurement. Lastly, the matching effects on the NF were analyzed. This analysis was done by introducing three impedance standards on the DUT to create different matching conditions. Under these circumstances, NF was measured at 5.63 dB, 5.76 dB, and 4.75 dB for 'SHORT', 'OPEN' and 'LOAD' impedance standards, respectively.

CHAPTER 1

INTRODUCTION

The evolution of wireless mobile communication from the 3^{rd} generation to the 4^{th} generation system creates strong demand for on-chip circuitry. Furthermore, the increasing pressure for lower power, higher integration and lower production cost in wireless communication market is another reason that drives the industry to move to on-chip solutions. Besides that, the current trend of Radio Frequency (RF) communication system is to produce smaller and low-noise wireless receiver circuitry, which necessitate an accurate NF measurement (Mohd. Noh and Zulkifli, 2006), (Mustaffa et al., 2008a), (Ramiah and Zulkifli, 2006). The NF performance of this wireless receiver is highly dependent on its components. In the architecture of the wireless receiver, the industry uses parallel components such as RF filters and Low-Noise Amplifier (LNA) at the front end of the receiver circuit, which shows that LNA is actually the backbone of the wireless receiver since it is the first gain stage in the receiver path. The main function of an LNA is to increase the level of input signal while minimizing the Signal-to-Noise Ratio (SNR) of the whole system at the same time (Mohd. Noh and Zulkifli, 2007), (Mustaffa et al., 2008b). Therefore, by considering the important function of an LNA, NF is one of the crucial parameters that need to be measured accurately.

Noise, is usually referred to as excitations of undesired signals affecting overall

system performance (Goo, 2001). On the other hand, NF (a measure of noise generated by a device) is one of the system parameters that characterize an ability of a system to process low level signals (Maury Microwave, 1999). One option for improving NF is to increase the transmitter power, which is very costly. Another option is to improve the LNA performance, which requires NF characterization. It is always more practical and easier to improve the LNA performance than to increase the transmitter power (Agilent, 2006).

1.1 Motivation

The ever-increasing demand for high frequency system and on-chip RF circuitry has brought about the need to measure a component directly on-wafer (Marzuki et al., 2005), (Beland et al., 1998). On-wafer NF measurement is essential for RF chips screening and design verification. Access to the device is normally done physically through a probe. However, parasitic associated with cables, connectors and probes contributes to inaccurate on-wafer NF measurement (Chen and Deen, 2001). Therefore, proper correction to eliminate these parasitic is crucial for a reliable NF result (Weng, 1995).

Several groups have reported their approaches to obtain an accurate on-wafer noise measurement. (Kantanen et al., 2003) and (Vaha-Heikkila et al., 2003) using a measurement system, which is based on cold-source method and computer controlled software to extract noise parameters. On the other hand, (Long et al., 2003), (Tiemeijer et al., 2005), (Chen et al., 2008) using a Y-factor method as a basis of on-wafer noise measurement system. However, the similarity of them is that they had used an expen-

sive tuner in the measurement setup to generate various source impedance. Several points of noise parameters were measured from these source impedance generated (Escotte et al., 1993). Optimization technique was then adopted to extract the four noise parameters based on method of least squares fit (Hu and Weinreb, 2004). The four noise parameters are the minimum NF, NF_{min}, noise resistance, R_n, and optimum impedance, Z_{opt}, or source admittance, Y_{opt} (Asgaran et al., 2007). These noise parameters are the function of source impedance and require measured NF data in order to form several linear equations. A minimum of four independent measurements are required to form the equations. However, more measurement will increase the accuracy of the results (Asgaran et al., 2006). From here, NF is then calculated using the noise parameters obtained based on the optimization techniques. This method is very time-consuming and requires an expensive tuner (Xiong et al., 2007). Furthermore, it is not a direct method to measure NF, where it needs to measure noise parameters first. Therefore, an accurate, tunerless, and direct method of NF measurement needs to be developed.

There are several methods available for measuring NF and the most common one is the classical Y-factor technique (Victor and Steer, 2005). The classical Y-factor technique is implemented in some high-end commercial NF characterization systems, in which only noise power measurements are involved (Tiemeijer et al., 2005), (Otegi et al., 2005b). However, because of the use of scalar noise power measurements alone, mismatch conditions in evaluating the noise performance of a device were ignored (Engen, 1973). The existence of mismatch in the measurement path would result in an error of the NF measurement (Adamski, 2000). A corrected Y-factor technique was proposed by combining the classical Y-factor method with scattering parameter mea-

surements (Collantes et al., 2002). Corrected Y-factor technique utilized an available gain (G_a) in the NF calculation through the use of vector measurement whereas classical Y-factor technique used an insertion gain (G_i) in NF calculations through the use of scalar measurement (Adamski, 2002). However, the comparison between G_a and G_i has never been discussed and as of now, the best gain definition to be used for the NF measurement is ambiguous.

At present, automated systems that perform NF and gain measurements are commercially available. Gain is measured by taking the ratio of noise output power as the device is being inserted and removed. Then, NF is calculated based on this ratio. It is an accurate NF measurement provided that all the elements involved are well matched, however, less concern was given to the mismatch associated with cables, connectors, probes, and noise sources (Di Paola and Sannino, 1999). Lack of knowledge on how the mismatch conditions influence NF is one of the reasons that contribute to an error during NF characterization.

1.2 Overview

This work focuses on the accurate method of on-wafer NF measurement. To achieve its goal, this thesis tackles several approaches to NF measurement such as tuner-less setup of on-wafer NF de-embedding procedures, gain uncertainty analysis, and the influence of impedance mismatch to the NF measurement. Chapter 1 in this thesis, deals with the introduction of this work and motivation for the thesis.

An overview about NF is given in Chapter 2. A brief explanation about NF theory

is presented, and the discussions are elaborated to the concept of NF and NF calculation for a multi-stage system. The fundamental principles on the NF measurement and standard method to measure NF are also covered in this chapter. The dependence of NF measurements on the noise linearity principle is shown together with an example of a simple NF measurement. Overall, Chapter 2 is about the fundamental of on-wafer NF measurement as it is important to understand the fundamental parts before going to the subsequent stages.

Chapter 3 highlights the methodology of on-wafer NF measurement. At the beginning of this chapter, basic elements involved in NF measurement experimental setup are discussed. Then, the chapter addresses the issue of on-wafer NF measurements and discusses the de-embedding method proposed. Besides that, other issues that influence the NF such as gain uncertainty and matching conditions are also covered in this chapter.

In Chapter 4, the implementation of the experimental procedures carried out are included. Detailed procedures as well as all the mathematical equations are provided. As for the comparative study, measurement procedures for the commercial LNA is also outlined. The measurement procedure for the de-embedding method as well as gain uncertainty analysis method is shown, which rely on the use of the conventional Noise Figure Analyzer (NFA) and Vector Network Analyzer (VNA). Semiconductor Parameter Analyzer (SPA) is used to supply and monitor Direct Current (DC) of a device.

Next, results and discussions are discussed in Chapter 5. Results of measurement

between the on-wafer NF measurement without the de-embedding and by including the de-embedding procedures are placed in comparison. The analysis of NF sensitivity to the gain uncertainty and the effect of NF to the device measured under various conditions have also been shown. Discussions on each observations are also conducted.

Finally, Chapter 6 concludes finding of this work. This chapter clearly specifies the accomplishment of this work. It also includes the future work that can be performed in order to further develop the research.

Additional to the seven chapters, MATLAB® programme and derivation of the equations used are included in the appendices. Besides that, some photos and an example of on-wafer measurement are also provided. These materials may help researchers of similar studies in doing the measurements and to further enhance their research.

CHAPTER 2

OVERVIEW OF NOISE FIGURE

The general definition of the word ‘noise’ in Oxford dictionary includes "pleasant and unpleasant sound" or "irregular fluctuations accompanying transmitted signals but not relevant to it" (Jewell, 2006). In the context of electronic circuitry, the second part of the definition above would be more relevant.

Noise is usually referred to as any undesired excitations to the system. In other words, noise is "everything except for the desired signal" (Goo, 2001). Sources of noise can either be internally or externally. There are various sources of external noise, which include: human voices, broadcasting signals that induce electromagnetic field, electric motors used in the industrial sector and home appliances, and also sources from nature such as lightning. Proper shielding is adequate in order to avoid these external noises from affecting the performance of an electronic circuits and devices.

A noise phenomenon generated within a device is known as an internal noise (Rogers and Plett, 2003), (Demir, 1997). Depending only on the shield protection is not sufficient enough to reduce the effect of the internal noise since the noise is inherent to a system or a device. Main sources of internal noise that are associated with Integrated Circuits (IC) are thermal noise, shot noise, flicker noise, burst noise and avalanche noise (Gray, 2001), (Refer to Appendix A for overview of these noises) (Carlson et al., 2002).

NF is a measure of noise generated by two-port devices. In other words, NF is also known as a parameter that characterizes the ability of a receiver to process low level signals. Once it is known, the sensitivity of the receiver can be estimated (Demir, 1997). In the context of spectrum analysis, the presence of noise in a wireless system is sometimes labeled as noise floor. The amplitude of a transmitted signal data must be higher than this noise floor for a successful wireless communication. Therefore, one option to improve NF is to increase the transmitter power, which is very expensive to implement and may even perhaps be illegal according to the law of the local government. The other approach is to lower the NF of an LNA considering it is the first gain stage in a receiver path as shown in Figure 2.1. LNA is a key component which is often positioned at the front-end of a receiver to ensure the received signals are quality enough for further processing (Au, 1998). Its main function is to provide gain amplification of the received signals, while at the same time minimizing overall NF attributed by the receiver stage. Due to this fact, LNA is one of the most important stages to be designed and hence, an accurate NF measurement becomes crucial (Mohd Noh, 2009), (Marzuki et al., 2004).

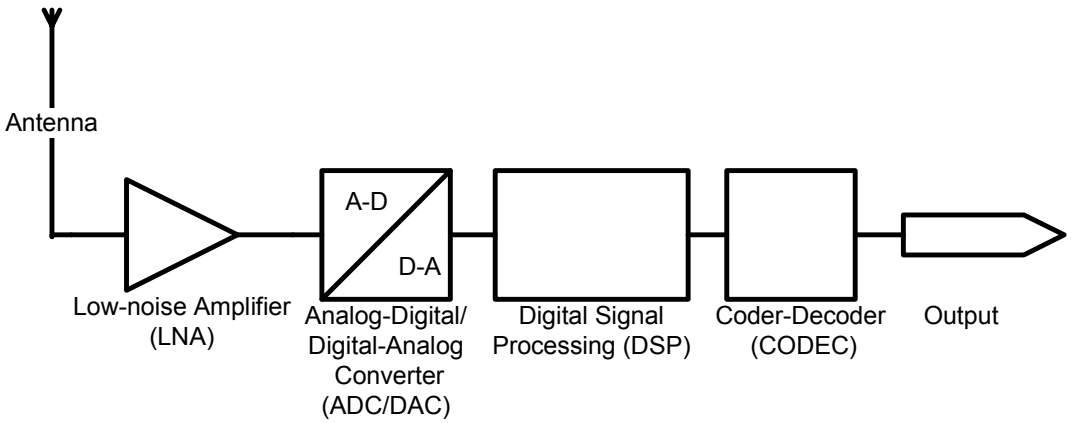

Figure 2.1: Ideal receiver.

2.1 Concept of Noise Figure

NF is a quantity used as a 'figure of merit' to describe the noise performance of a device. It came into popular use in 1944, when Harold Friis defined the terms. Noise Factor (F) is a numerical ratio of NF, where NF is expressed in dB. Hence,

$$NF = 10logF. \tag{2.1}$$

F is defined as SNR at the input (S_i/N_i) to the SNR at the output (S_o/N_o). The available signal power at the input (S_i) and available noise power at the input of a device (N_i), represent signal and noise at the input, whereas available signal power at the output (S_o) and available noise power at the output of a device (N_o), represent signal and noise at the output, respectively (Friis, 1944). Basically in a wireless receiver, a perfect amplifier would amplify both the received signals as well as the noise, while maintaining the SNR at its input and output at the same time. However, in any real characterization setup, the amplifier itself would also add some extra noises of its own. These extra noises are actually the NF of the amplifier. Refer to the following explanations, which are based on illustrations shown in Figure 2.2 and 2.3 to best describe the above statement (Agilent, 2006).

Figure 2.2 shows an example of input signal of an amplifier, which indicates about 40 dB above noise floor. On the other hand, Figure 2.3 shows an example of output signal of the amplifier, which has been amplified by 20 dB. However, the amplifier has also added its own noise, which is about 10 dB more. Therefore, the output signal observed is only 30 dB above the noise floor. In this case, the degradation in signal-to-

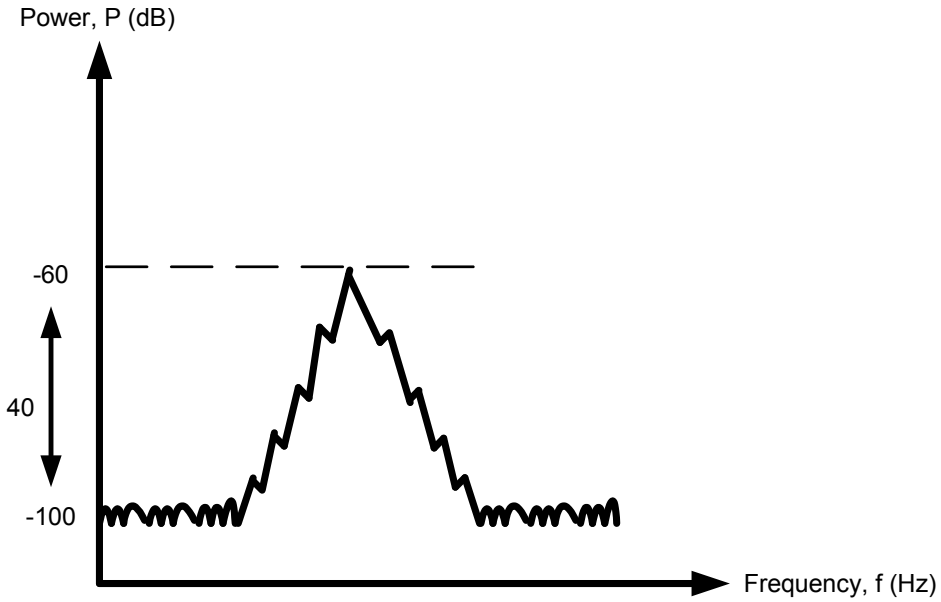

Figure 2.2: Example of amplifier input power.

noise ratio is 10 dB. The 10 dB is actually the NF of the amplifier.

2.1.1 Noise Figure of a Two-Port Device

An example of a linear two-port device is shown in Figure 2.4.

Based on the definition of F from Section 2.1, the NF equation of a two-port device is written as (Engberg and Larsen, 1995),

$$F = \frac{S_i/N_i}{S_o/N_o}. \tag{2.2}$$

In Figure 2.4,

$$S_o = GS_i, \tag{2.3}$$

and,

$$N_o = N_a + GN_i, \tag{2.4}$$

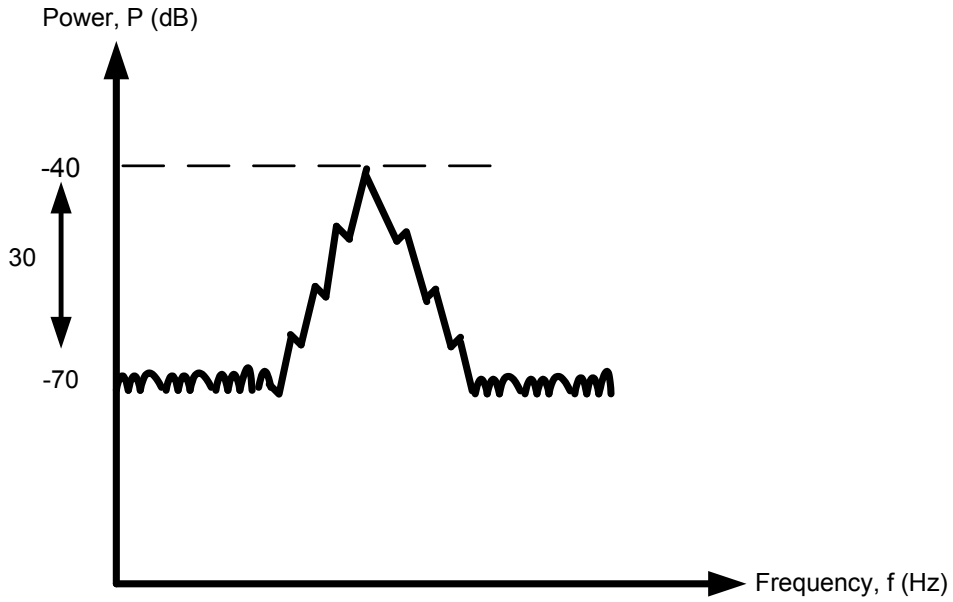

Figure 2.3: Example of amplifier output power.

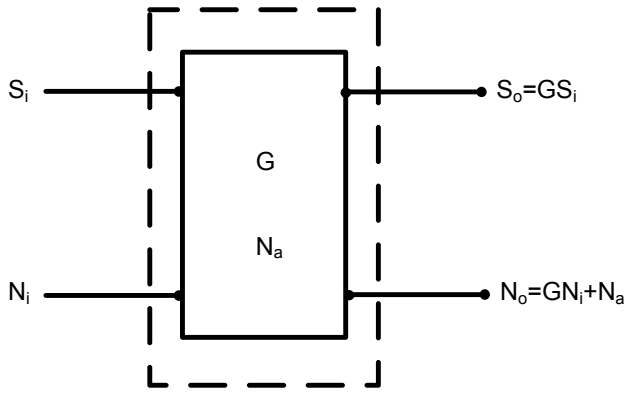

Figure 2.4: Linear two-port device.

where noise power added by a device (N_a) and gain (G), are the noise added and gain of a two-port device, respectively. Substituting Equation 2.3 and 2.4 into Equation 2.2,

$$F = \frac{S_i/N_i}{GS_i/(N_a + GN_i)}. \tag{2.5}$$

Leading to,

$$F = \frac{N_a + GN_i}{GN_i}, \tag{2.6}$$

N_i is actually a thermally available noise power at the input and is referred to by,

$$N_i = kT\Delta f, \tag{2.7}$$

where k is Boltzmann's constant and is equal to $(1.38 \times 10^{-23})(J/K)$, Δf is the change of bandwidth and T is the temperature expressed in Kelvin.

Therefore, Equation 2.6 can be written as,

$$F = \frac{N_a + kT\Delta fG}{kT\Delta fG}, \tag{2.8}$$

2.1.2 Noise Figure of a Multi-Stage System

Multi-stage system is an arrangement of several individual stages in series. An example of multistage system is a receiver module, which consists of an antenna, LNA and other components as illustrated in Figure 2.1. The NF of a multi-stage system can be best explained using a diagram shown in Figure 2.5.

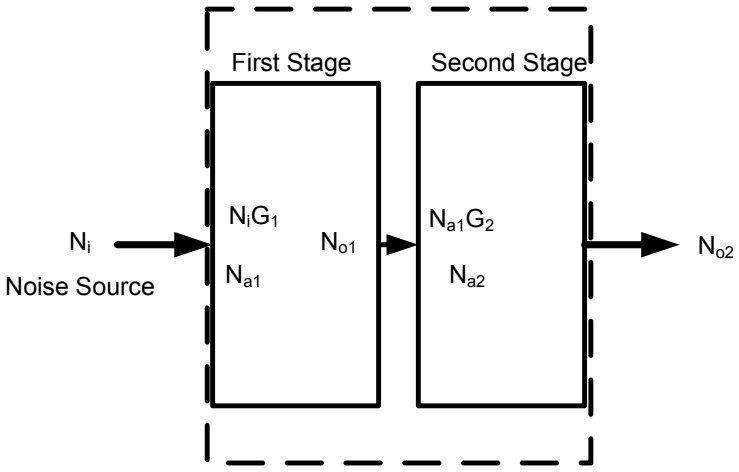

Figure 2.5: Example of multiple-stage system.

Information about the NF of a multi-stage system relies on the knowledge of the NF of each individual stage. It is based on the cascade equation, which is derived below. In Figure 2.5, a multi-stage system can be treated as a black box, which is illustrated as a dotted box. Therefore, a derivation can be made by making a reference to Section 2.1.1. Overall noise factor of all the stages (F_{all}) is then obtained by solving all the unknown in the equation.

In Figure 2.5, F_{all} can be attained by the knowledge of available noise power at the output for the second stage (N_{o2}). N_{o2} is derived using the method shown in (Davis and Agarwal, 2001). However, it is started by having the knowledge of available noise power at the output for the first stage (N_{o1}). In Figure 2.5, N_{a1} is the noise power added by a device in the first stage, N_{a2} is the noise added by a device in the second stage, G_1 is the gain of the first stage and G_2 is the gain of the second stage. From Equation 2.4 and 2.7, N_{o1} can be written as,

$$N_{o1} = N_{a1} + G_1 N_i = kT\Delta f G_1 (F_1 - 1) + G_1 kT\Delta f. \tag{2.9}$$

N_{o2} is then calculated by multiplying N_{o1} and gain of the second stage (G_2), which gives,

$$N_{o2} = N_{a2} + G_2 N_{o1} \tag{2.10}$$

Therefore, by adopting Equation 2.9 to the Equation 2.10 the equation reads,

$$N_{o2} = N_{a2} + N_{a1} G_2 + G_1 G_2 N_i, \tag{2.11}$$

Rearranging Equation 2.8 and substituting it into Equation 2.11 gives,

$$N_{o2} = kT\Delta f G_2(F_2 - 1) + kT\Delta f G_1 G_2(F_1 - 1) + kT\Delta f G_1 G_2, \tag{2.12}$$

leading to,

$$N_{o2} = kT\Delta f G_1 G_2(F_1 + \frac{F_2 - 1}{G_1}). \tag{2.13}$$

From here, F_{all} is obtained by adopting Equation 2.6, 2.4 and 2.13, since GN_i is equal to $kT\Delta f G_1 G_2$,

$$F_{all} = \frac{kT\Delta f G_1 G_2(F_1 + \frac{F_2 - 1}{G_1})}{kT\Delta f G_1 G_2} = F_1 + \frac{F_2 - 1}{G_1}. \tag{2.14}$$

Equation 2.14 is known as the cascade equation. By performing the same methodology, the cascade equation can be further extended up to several stages, as long as the components composed in the multi-stage system are in series. The observation made from this cascade equation is that whenever the gain of the first stage is high, noise contributions from the second stage and so on will be small. Therefore, in any wireless communication system, gain of the first stage must be high in order to reduce the overall NF of the system.

2.2 Fundamentals of Noise Figure Measurement

This section gives an insight regarding the fundamentals of the NF measurement. The NF measurement relies on the principle of noise linearity. In noise linearity, N_o of a device is dependent on the amount of N_i, which has been stimulated to the input port of the device. N_o is proportional to N_i as shown in Figure 2.6. N_a on the other

hand, is not influenced by N_i or N_o. N_a comes solely from the device. Therefore, no matter how much the amount of noise is stimulated to a device, N_a remains the same. By manipulating this kind of behavior, NF of a device can be obtained. N_i is actually thermally available noise power at the input, which is generated by a noise source. In Figure 2.6, a larger amount of noise power at the input N_i, is generated as the temperature of noise source increases.

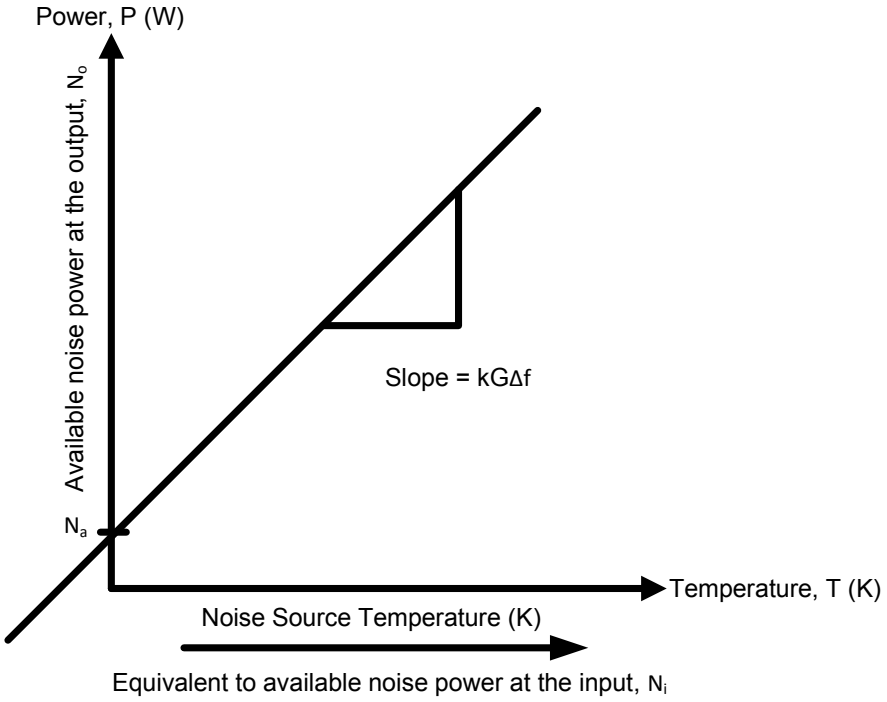

Figure 2.6: Graph plot to represent noise linearity (Agilent, 2004).

From Figure 2.6, the NF is obtained by adopting a well-known straight line equation, $y = mx + c$. In this case, the slope of the graph (m) represents $kG\Delta f$, whereas the intercept points at y-axis (c), y-axis (y) and x-axis (x) represent N_a, N_o and temperature (K) (T), respectively. The substitution of the straight line equation with the equivalent NF representation gives,

$$N_o = kG\Delta fT + N_a, \tag{2.15}$$

which corresponds to Equations 2.4 and 2.7. From here, Equation 2.15 is substituted into Equation 2.6, which finally leads to NF after applying Equation 2.1. The advantage of using the noise linearity principle in NF measurement is that, by having two levels of N_i, two levels of N_o can be produced. Then, noise linearity graph plot is realized. Therefore, one simple mechanism to have these two levels of N_i is by turning 'ON' and 'OFF' the noise source. Noise source generates a small amount of noise during its 'OFF' state, which is always referred as the temperature of noise source during the 'COLD' state (K) (T_c) since there is no voltage that turn on the diode located inside the noise source. Then, larger amount of noise during its 'ON' state, which is referred as the temperature of noise source during the 'HOT' state (K) (T_h), since there is voltage that turn on the diode this time.

2.2.1 The Y-Factor Method

Y-factor method is the most widely used procedure for the NF measurement (Collantes et al., 2002). The Y-factor method requires measuring the two levels of N_o for the two levels of N_i stimulated. The ratio of these two N_os is called as the Y-factor (Geens and Rolain, 2001). Y-factor can be represented by, (Garelli et al., 2009)

$$Y = \frac{N_2}{N_1}, \tag{2.16}$$

where noise output power during the 'COLD' state (N_1) and noise output power during the 'HOT' state (N_2) are the two levels of the measured N_o. The derivation of Y-factor methodology that leads to NF is best explained using the illustration shown in Figure 2.7 (Jasper, 2010).

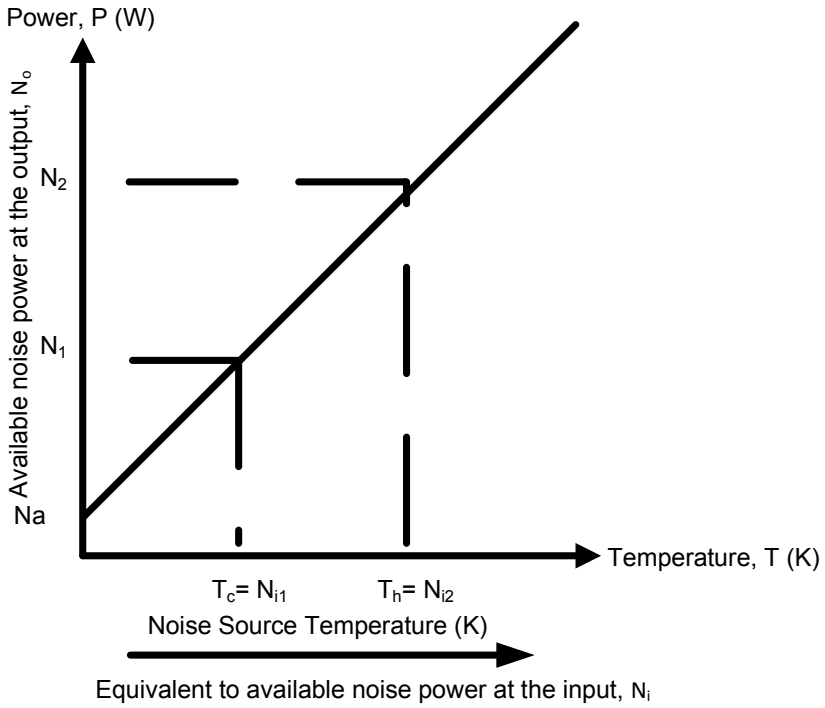

Figure 2.7: Graph plot for the y-factor method.

N_1 and N_2 are measured while stimulating small amount of thermal noise during the 'COLD' state (N_{i1}), and large amount of thermal noise during the 'HOT' state (N_{i2}). Based on these values, the noise linearity as in Figure 2.7 is plotted. The slope which is $kG\Delta f$, is calculated as follows:

$$\frac{N_2 - N_1}{T_h - T_c} = kG\Delta f. \tag{2.17}$$

Combining Equation 2.15 and Equation 2.6 give,

$$F = \frac{N_o}{GN_i}. \tag{2.18}$$

Substituting Equation 2.7 and by the assumption that N_o is represented by N_1 and N_2, Equation 2.18 becomes,

$$F = \frac{N_2}{kGT_h\Delta f} = \frac{N_1}{kGT_c\Delta f}. \tag{2.19}$$

Then, by combining Equation 2.17 with Equation 2.19 this leads to,

$$F = \frac{N_1}{T_c}(\frac{T_h - T_c}{N_2 - N_1}) = (\frac{T_h - T_c}{T_c})(\frac{N_1}{N_2 - N_1}). \tag{2.20}$$

Adopting Equation 2.16,

$$\frac{1}{Y-1} = \frac{N_1}{N_2 - N_1}, \tag{2.21}$$

and,

$$ENR = \frac{T_h - T_c}{T_c}, \tag{2.22}$$

where will be explained in the next chapter. Therefore, the F equation that leading to NF based on Y-factor method can be written as

$$F = \frac{ENR}{Y-1}. \tag{2.23}$$

Noted that in the Y-factor method, only scalar power measurements are involved.

2.2.2 Overview of Noise Figure Measurement

An example of a simple NF measurement setup is shown in Figure 2.8. It is a two-stage cascaded system, which is composed of Device Under Test (DUT) and NFA. Utilizing Equation 2.14 and assume that DUT is the first stage of the system whereas NFA is the second stage, Equation 2.14 is now written as,

$$F_{all} = F_{DUT} + \frac{F_{NFA} - 1}{G_{DUT}}. \tag{2.24}$$

In Equation 2.24, the noise factor of the device under test (F_{DUT}) and gain of the device under test (G_{DUT}) represents the noise factor of the first stage (F_1), and gain of the first stage (G_1), whereas the noise factor of the noise figure analyzer (F_{NFA}) represents the noise factor of the second stage (F_2), respectively.

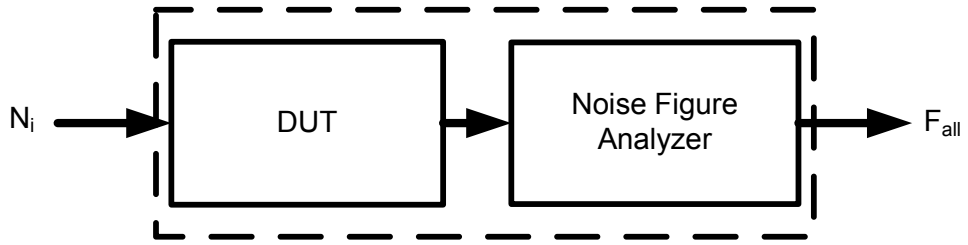

Figure 2.8: The block diagram of the NF measurement system.

To get F_{DUT}, Equation 2.24 needs to be rearranged as follows:

$$F_{DUT} = F_{all} - \frac{F_{NFA} - 1}{G_{DUT}}. \tag{2.25}$$

In Equation 2.25, F_{DUT} is equal to F_{all} only if the G_{DUT} is large enough in order to eliminate the second term. Otherwise, the knowledge of F_{NFA} is required to accurately calculate F_{DUT}. F_{NFA} in Equation 2.25 can be measured by directly connecting the noise source to the NFA as shown in Figure 2.9. Figure 2.10 shows a block diagram for such a connection. It is the same as the calibration setup. After calibration, NFA holds the F_{NFA} value. During the actual measurement, NFA will automatically subtract F_{NFA} and only displays the value of F_{DUT}.

F_{all} and G_{DUT}, are measured using the illustration shown in Figure 2.11, which is based on the Y-factor method. The NF of the DUT can be calculated by substituting F_{NFA}, F_{all}, and G_{DUT} into Equation 2.25.

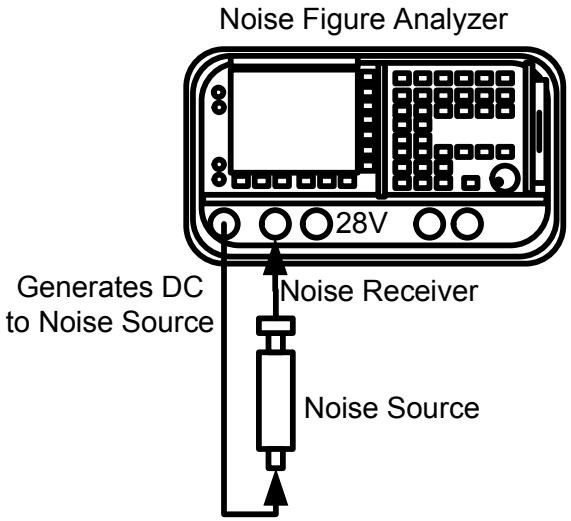

Figure 2.9: Connecting noise source to the NFA directly.

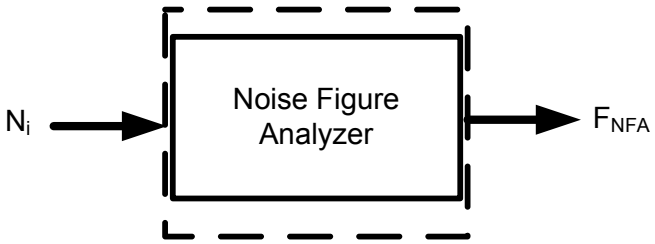

Figure 2.10: The NF of the NFA's determination.

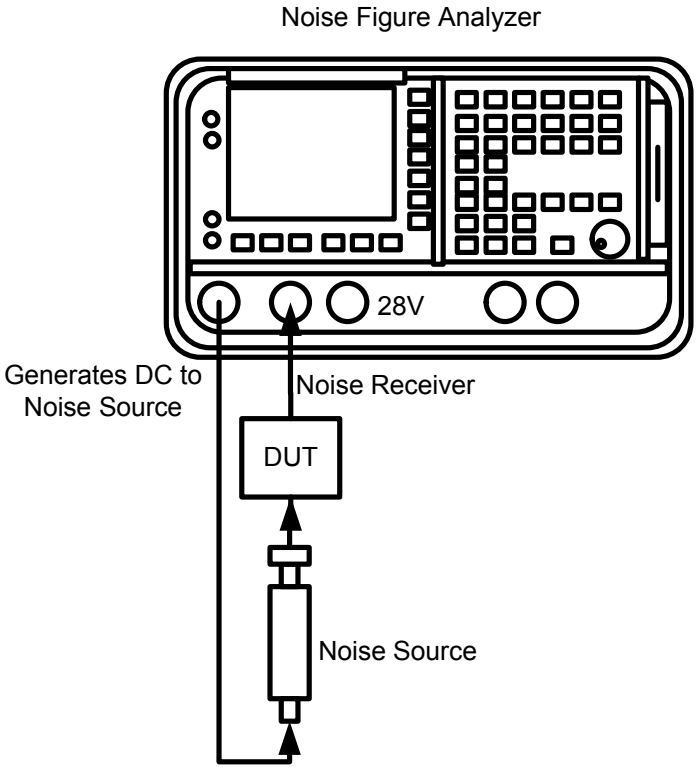

Figure 2.11: The NF measurement of the DUT.